Stray current induced corrosion of steel fibre reinforced concrete

Kangkang Tang

kangkangtang@gmail.com

Faculty of Science and Engineering, University of Wolverhampton, UK

Abstract

Stray current induced corrosion is a major technical challenge for modern electric railway systems. The leakage of stray current to surrounding reinforced concrete structures can lead to steel reinforcement corrosion and the subsequent disintegration of concrete. Steel fibre reinforced concrete has been increasingly used as the railway tunnel lining material but it is not clear if discrete steel fibres can still pick up and transfer stray current in the same way as conventional steel reinforcement and lead to similar corrosion reactions. The corrosion behaviour of steel fibres was investigated through voltammetry tests and electrochemical impedance spectroscopy. The presence of high concentration chloride ions was found to increase the pitting corrosion tendency of steel fibres in simulated concrete pore solutions and mortar specimens. The chloride threshold level for corrosion of steel fibres in concrete is approximately 4% NaCl (by mass of cement) which is significantly higher than that of conventional steel reinforcement.

Keywords: Steel fibre reinforced concrete; EIS; Cyclic voltammetry; Potentiostatic; Passivity; Pitting corrosion

List of notations

α_a, α_c Constant values (V)

A Exposed anode area (cm^2)

β_a, β_b Anodic and cathodic Tafel constants/gradients

C_f Capacitance of mortar ($S \cdot s^n \cdot cm^{-2}$)

C_{dl} Capacitance represents the layer between the solution and the steel surface. Faradaic charge transfer reaction on the steel surface ($S \cdot s^n \cdot cm^{-2}$)

CR Corrosion rate (mm/year)

EW Mass of metal that will be oxidized by the passage of one Faraday of electric charge (27.925 for steel)

$E_{e,a}$, $E_{e,c}$ Anodic and cathodic equilibrium potentials (V)

E_{corr} Corrosion potential (V)

I Measured current from the circuit or the net electron flow (A)

I_a, I_c Anodic and cathodic currents (A)

$I_{0,a}$, $I_{0,c}$ Anodic and cathodic exchange currents (A)

I_{corr} Corrosion current (A)

i_{corr} Corrosion current density (A/cm^2)

K Constant value: 3.27×10^{-3} ($mm \cdot g/\mu A \cdot cm \cdot year$)

L Distance between substations (km)

$\eta_{e,a}$, $\eta_{e,c}$ Anodic and cathodic overpotentials (V) from the equilibrium potential $E_{e,a}$ and $E_{e,c}$

ρ Density (7.8 g/cm^3 for steel)

r_R Resistance of the running tracks (Ω/km)

r_T Track-earth resistance (Ω·km)

R_S Resistance of the solution (kΩ·cm^2)

R_f Resistance of mortar layer (kΩ·cm^2)

R_{ct} Charge transfer resistance of the steel (kΩ·cm^2)

θ Phase shift (radian)

W Warburg diffusion element (S·s$^{1/2}$·cm^{-2})

~~1.~~1 Introduction

Railway electrification represents an important carbon strategy in the UK. It is estimated that an electric train consumes at least 20% less power (per passenger per mile) compared to a diesel-powered train [1]. In the UK, only 39% of the national rail network is electrified and it comprises 600 V/750 V direct current (DC) and 25 kV (50 Hz) alternating current (AC) traction power systems [2]. The UK government is committed to promote railway electrification and thus provide more sustainable and comfortable services for the public. Major work has been carried out for the Crossrail project which is expected to be delivered in 2018 and the construction of High Speed 2 (HS2) is expected to begin in 2017. In addition, the planning stages for HS3 and Crossrail 2 projects are both underway. For a modern electric train traction system, the transmission of power is normally provided by an overhead wire or a conductor rail. The return circuit is usually through the running tracks which are connected to nearby substations. Stray current refers to the current which disperses directly to the ground through the return path. Niasati and Gholami [3] proposed a simplified electronic circuit of the electric railway system, as shown in Fig. 1-(a), to model the stray current leakage. In this circuit, stray current (i_S) can be determined according to railway traction current (i_T), resistance of the running tracks (R_R) and the track-earth resistance (R_T) based on Eq. (1). The resistance of the overhead catenary wire (R_C), in comparison to that of the running tracks (R_R), is negligible and it has not been taken into account in Eq. (1).

$$i_S = \frac{R_R i_T}{R_T + R_R + R_S} \quad \textbf{(1)}$$

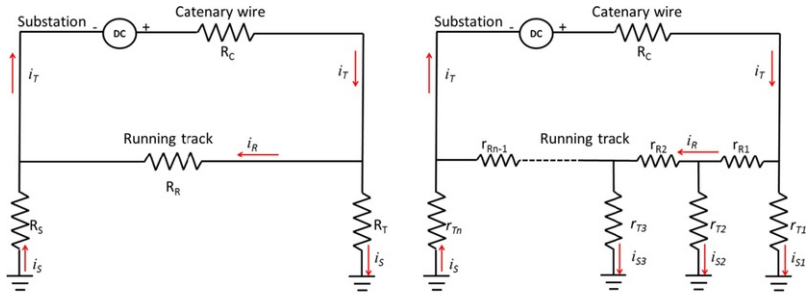

~~Fig. 1.~~Fig. 1 Equivalent electronic circuits of stray current formation.

alt-text: Fig. 1

Considering a more general condition that more than one leakage of stray current occurs along the running tracks, as shown in Fig. 1-(b), Eq. (2) can be used to quantify stray current (i_S). r_R represents the resistance of the running tracks and r_T represents the track-earth resistance [4].

$$i_S = \frac{1}{12} i_T \frac{r_R}{r_T} L^2 \quad \textbf{(2)}$$

Both Eqs. (1) and (2) indicate that reduced track-earth resistance (R_T or r_T) will encourage traction current leakage or stray current (i_s). The leakage of stray current to surrounding structures, e.g. reinforced concrete sleepers and tunnel linings (Fig. 2), can lead to steel reinforcement corrosion and the subsequent disintegration of concrete which eventually reduces the service life of the entire railway system [5–7]. Stray current also accelerates the corrosion of underground service cables, water mains and gas pipes. Approximately £550 million is required per annum for the rehabilitation and repair of the stray-current induced corrosion damage to the UK infrastructures [8]. It is engineering practice to mitigate against stray current by providing sufficient insulation between the running tracks and earth, i.e. to increase R_T or r_T. The use of a separate rail (or the fourth rail) as the return circuit as used by some London underground subway lines can also effectively reduce the magnitude of stray current, but the cost of installing and maintaining the fourth rail over the entire design life of a railway system is significant. It should be noted that increased resistance of running tracks (R_R or r_R) can also lead to an increased stray current according to Eqs. (1) and (2). The rail track joints are therefore required to be either welded or using low resistance joint bonds, complying with BS EN 50122-2 [9]. Reducing the distance between adjacent substations (L) can effectively reduce stray current although this has a cost consequence too. A stray current collection system, complying with BS EN 50122-2:2010 [9], can capture the stray current and return it back to substations through a return earth wire [10]. This can also be taken as an effective stray current mitigation method.

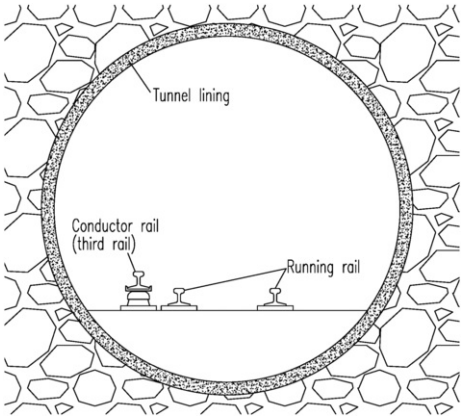

~~Fig. 2.~~Fig. 2 Schematic of the railway tunnel section.

alt-text: Fig. 2

The corrosion of conventional steel reinforcement in concrete is often of an electrochemical nature. The corrosion process consists of at least two half-cell reactions, i.e. an oxidation reaction at the anode (loss of electron) and a reduction reaction at the cathode (gain of electron) [11]. The anodic reaction is normally iron dissolution:

$$Fe \rightarrow Fe^{2+} + 2e^{-} \quad \textbf{(3)}$$

The cathodic reaction can be oxygen reduction:

$$O_2 + 2H_2O + 4e^{-} \rightarrow 4OH^{-} \quad \textbf{(4)}$$

The cathodic reaction can also be water reduction, in the absence of oxygen:

$$2H_2O + 2e^{-} \rightarrow 2OH^{-} + H_2 \quad \textbf{(5)}$$

Negatively charged electrons released from the anode travel to the cathode through the steel reinforcement. The formation of electrochemical cells also requires a continuous path for ions between the anode and the cathode which normally occurs through the concrete pore solution. Steel corrosion or oxidization is primarily a result of the anodic current (I_a) according to Faraday's laws of electrolysis, i.e. the amount of substance which reacts or literates is directly proportional to the quantity of electric charge passing through it. Corrosion normally occurs at an equilibrium state between the two half-cell reactions, upon which anodic and cathodic currents are both present and equal to each other, namely the corrosion current (I_{corr}) [12]. The steel corrosion rate (CR) can be determined according to Eq. (6) [13]:

$$CR = \frac{K I_{corr} EW}{\rho A} \quad \textbf{(6)}$$

The corrosion rate (CR) can also be determined based on a weight loss measurement, i.e. the loss of weight as a function of time. This gravimetric method is however more appropriate for uniform corrosion damage rather than pitting corrosion (or pitting) which is a common form of steel reinforcement corrosion but without inducing significant mass change [14].

The corrosion current (I_{corr}) can be determined by conducting a linear sweep voltammetry test where the current (I) at a working electrode (WE) is measured while an externally applied potential (E) is swept between the WE and a reference electrode (RE). This is due to the linear correlation between the overpotential (η) and the logarithm of the measured current (I) when the electrochemical reaction speed is controlled by the kinetics of electron transfer [15]. This correlation is also called Tafel behaviour which can be described as Eq. (7):

$$\eta_a = \mathrm{E} - E_{e,a} = \alpha_a + \beta_a \ln I_a \quad \textbf{(7)}$$

Analogously, Tafel behaviour for the cathodic reaction can be described as:

$$\eta_c = \mathrm{E} - E_{e,c} = \alpha_c - \beta_c \ln I_c \quad \textbf{(8)}$$

Eqs. (7) and (8) can be written in an exponential format [16]:

$$I_a = I_{0,a} \exp\left(\frac{\mathrm{E} - E_{e,a}}{\beta_a}\right) \quad \textbf{(9)}$$

$$I_c = I_{0,c} \exp\left(-\frac{\mathrm{E} - E_{e,c}}{\beta_c}\right) \quad \textbf{(10)}$$

The corrosion current (I_{corr}) refers to the anodic or the cathodic current at the equilibrium state or $I_a = I_c$. There is therefore no net electron flow from the corrosion system as anodic and cathodic reactions are at the same speed. Eq. (11) or Butler-Volmer equation can be used to calculate the net electron flow (I) of an electrochemical cell [17]:

$$I = I_a - I_c = I_{corr}\left[\exp\left(\frac{\mathrm{E} - E_{corr}}{\beta_a}\right) - \exp\left(-\frac{\mathrm{E} - E_{corr}}{\beta_c}\right)\right] \quad \textbf{(11)}$$

Butler-Volmeter equation allows the determination of I_{corr} based on a regression analysis between the externally applied potential (E) and the measured current (I) [12]. The corrosion current (I_{corr}) can also be determined according to Stern-Geary equation (Eq. (12)) which is a mathematically reduced form of Butler-Volmeter equation [18].

$$I_{corr} = \frac{\beta_a \beta_c}{\beta_a + \beta_c} \times \frac{1}{R_p} \quad \textbf{(12)}$$

where R_p is the linear polarization resistance (LPR) which can be taken as the slope of an E-I plot when conducting a linear potential sweep near the E_{corr} (e.g. ± 10 mV). Eq. (12) can be further reduced to Eq. (13) and a constant B value can be used to quickly determine the corrosion current (I_{corr}) [11].

$$I_{corr} = \frac{B}{R_p} \quad \textbf{(13)}$$

Eq. (13) has been widely used in civil engineering projects to give a rapid corrosion evaluation of steel reinforcement as it does not require measurements of the other electrokinetic parameters such as Tafel constants [19–21]. It should be noted that the validity of Stern-Geary equation or its reduced form (Eq. (13)) still depends on the Tafel behaviour of the anodic and cathodic reactions. They may lead to an inaccurate prediction of the corrosion current (I_{corr}) for a diffusion-controlled (or diffusion-limited) corrosion reaction. In this work, a regression analysis based on Butler-Volmer equation (Eq. (11)) was conducted to determine I_{corr}.

In addition to the voltammetry test, electrochemical impedance spectroscopy (EIS) has been widely used to determine the corrosion susceptibility of steel reinforcement in concrete by measuring its electrochemical impedance (Z) [22–26]. This is achieved by applying a small sinusoidal potential, $E_0 \cdot \sin(\omega t)$, to an electrochemical cell. The cell's current response, $I_0 \cdot \sin(\omega t + \theta)$, is also sinusoidal but with a phase shift (θ). Z can be calculated and presented in following form [27]:

$$Z = \frac{E}{I} = \frac{E_0 \cdot \sin(\omega t)}{I_0 \cdot \sin(\omega t + \theta)} = \frac{E_0}{I_0}(\cos\theta + j \cdot \sin\theta) \quad \textbf{(14)}$$

EIS results can be presented in a Nyquist or a Bode plot. In the Nyquist plot, the imaginary impedance (Z') is plotted against the real impedance (Z) at each excitation frequency. In the Bode plot, θ is plotted on the Y-axis with the frequency on the X-axis. It is engineering practice to interpret EIS data through equivalent electronic circuit modelling [28]. An equivalent electronic circuit model may consist of resistors, capacitors and inductors which have different physical meanings. John et al. [19] developed an equivalent circuit model consisting of resistors and capacitors to represent electrochemical interfaces in a reinforced concrete specimen. The capacitor represents the double layer at the electrode (i.e. steel reinforcement) surface and the resistor represents the electrode and solution resistance. Reinforcement corrosion in concrete can however be complicated due to the change of the steel-concrete interface conditions as a result of the formation and breakdown of the steel passive layer. The interpretation of EIS data using a single equivalent circuit over a long period of time may therefore be inaccurate. Wei et al. [26] proposed

four different electronic circuits to represent different steel-concrete interface conditions, e.g. from steel in a passive state to an accelerated corrosion process controlled by mass transfer. EIS results can provide in-depth information on charge transfer kinetics such as charge transfer resistance (R_{ct}) which is directly relevant to the susceptibility of steel pitting corrosion in concrete.

Steel reinforcement corrosion is mainly a result of the anodic current (I_a) as discussed. An externally applied potential (E) can further push the anodic potential away from the equilibrium state and accelerate the anodic reaction (or corrosion) rate. Anodic overpotential (η_a) is therefore the major driving force for steel corrosion in concrete. It should be noted that high overpotential (η_a) does not always lead to a high anodic current (I_a). Steel, under alkaline conditions, can exhibit a passive behaviour (or passivation). Passivation leads to a decreased I_a even when E is increased. In concrete, the alkaline conditions (pH values between 12.5 and 13.5) are primarily provided by the calcium hydroxide as a result of cement hydration reactions. Chloride ions in the electrolyte help to break down the passive layer and lead to localized corrosion or pitting [29]. The influence of chloride ions on the passive layer was described by Saremi et al. [30] as a competing process between hydroxide and chloride ions which coexist in the concrete pore solution. Pitting only occurs when the disruptive effect of chloride ions overcomes the effect of hydroxide ions which stabilize the surface lattice of steel.

The presence of chloride in concrete can be a result of contaminated aggregate and water used during concrete mixing. The ingress of chloride from the external environment, e.g. de-icing agents, can also reach steel reinforcement through the concrete cover. The chloride threshold for the corrosion of conventional steel reinforcement in concrete is reported to be between 0.15 and 0.6% by mass of cement [31]. It should be noted that chloride exists in two different forms in concrete, i.e. free and bound chloride. Aguirre-Guerrero et al. [20] reported that bound chloride is chemically or physically attached to the cement hydration products and only free chloride ions in the concrete pore solution are responsible for the depassivation of steel reinforcement. Free chloride ions in the concrete pore solution can be measured by squeezing concrete samples at a high pressure [32]. Wan et al. [33] reported that 0.12 mol/L (or 7332 mg/L) free chloride was measured in the concrete pore solution obtained from a concrete specimen containing 0.5% of NaCl (by mass of cement). Shi et al. [34] reported that 0.3 mol/L NaCl solution could represent the free chloride concentration in the concrete pore solution under normal working conditions. 1 mol/L NaCl solution represents the chloride concentration in the concrete pore solution under severe marine environments. These studies also generate data that allow the use of simulated concrete pore solutions as the electrolyte to investigate the corrosion behaviour of steel reinforcement in concrete. As an example, Moser et al. [35] studied chloride induced corrosion resistance of stainless steel in simulated concrete pore solutions. NaCl was added into the simulated solutions at different concentrations. 0.5 mol/L NaCl was used to represent a concrete specimen in direct contact with seawater. Shi et al. [34] investigated the influence of chloride on the pitting corrosion resistance of steel reinforcement using simulated concrete pore solutions. Cyclic polarization tests were conducted to steel exposed to the simulated pore solutions using various NaCl concentrations, i.e. 0.1, 0.3 and 1 mol/L. 1 mol/L represents severe marine environments for characterization of pitting corrosion resistance.

Positively charged steel ions, as a result of the anodic reaction (Eq. (3)), can be hydrated and then oxidized to form hydrated ferric oxide (or rust). Rust developed on the steel surface will occupy a larger volume and lead to cracking and spalling of concrete cover due to internal pressure [29]. Unlike conventional steel reinforcement in concrete, there might not be a continuous conductive path for an electric current to be picked up by discrete steel fibres randomly dispersed within concrete. Sadeghi-Pouya et al. [36] conducted an accelerated corrosion test by applying a constant DC current (3A) to steel fibre reinforced concrete (SFRC) specimens, with a steel fibre content of 40 kg/m^3 and NaCl content of 3% (by mass of cement). The specimens were submerged in the NaCl solution and a titanium wire and a steel bar were respectively embedded into the specimen as the anode and cathode. There was no cracking or spalling observed on the surface of the concrete specimens after a month which represents a 60-year service life as required for ordinary building structures. The compressive strength and tensile splitting strength of the specimens were not jeopardized by the externally applied DC current either. Nemegeer et al. [37] cast concrete cubes comprising of different types of steel fibres and exposed them to the chloride solution for 18 months. Rusty stains were only identified on the surface of concrete containing steel fibres although no detrimental effect on the compressive strength of the concrete was observed.

Based on above information, SFRC appears to be an ideal substitute for conventional steel reinforcement in electric railway projects, with less concern about stray current induced corrosion. The use of SFRC also facilitates the concrete fabrication process by eliminating the need for constructing steel reinforcement cages. The structural function of railway tunnel segments is primarily to support the downward action from soil and buildings above the tunnel crown. From a structural perspective, the compressive strength of tunnel segments is of the upmost importance to ensure the overall stability of the tunnel. Velayutham et al. [38] reported that a steel fibre content equivalent to 40 kg/m^3 contributed to a significant increase in the 28-day compressive strength from 45.2 to 61.7 MPa. This finding agrees with Caratelli et al. [39] who reported an average compressive strength of 61.2 MPa achieved in concrete lining segments containing 40 kg/m^3 steel fibres. Randomly dispersed steel fibres in concrete also effectively restrain crack growth and reduce the permeability of concrete. Fire in a railway tunnel may lead to significant loss of life and long-time transport interruption. The presence of steel fibres was found to effectively enhance the fire resistance of concrete [40] and this further defines its advantage in the application in railway projects. The first large-scale application of SFRC segments in railway projects, without using any conventional steel reinforcement, was the 20 km twin-tube sections of the Channel Tunnel Rail Link project [41].

Solgaard et al. [42] however believed that corrosion of steel fibres may not be solely an aesthetical problem for SFRC. This was based on the electrochemical studies of mortar specimens (40 × 40 × 160 mm) containing two steel fibres (35 mm long and 0.55 mm in diameter) with a gap of 10 mm along their length. A linear polarization resistance (LPR) test was conducted to determine the corrosion rate (CR) of steel fibres according to Eq. (13). With up to 6% $CaCl_2$ (by mass of cement) added to the mix, steel fibres demonstrate a good resistance to chloride attack as no detrimental effect on the corrosion rate (CR) was observed. These specimens were then exposed to a constant DC current (1.2 mA) for 60 ~~hours~~h to simulate the stray current effect. The DC current, in conjunction with the presence of chloride, significantly increased the corrosion rate of steel fibres by two orders of magnitude. A reduced cross-

section area in steel fibres, as a result of corrosion reactions, may lead to reduced tensile strength of concrete which is essential to ensure the integrity of precast lining segments for future maintenance (e.g. when topsoil and subsoil is excavated) or other applications where it is beneficial to consider the tensile capacity of SFRC. The '*Guangzhou Metro Line 3*' project in China aimed to use SFRC as the primary lining material but this plan was eventually rejected because of the perceived uncertainties caused by stray current induced corrosion [43]. The primary objective of this work is to achieve a better understanding of the corrosion susceptibility of SFRC under stray current environments. This will enable the uncertainties concerning the pitting corrosion initiation and the corrosion rate (*CR*) measurement in SFRC to be clarified which will pave the way for the application of SFRC in electric railway projects.

~~2.~~2 Experimental procedures

Previous research on stray current induced corrosion of reinforced concrete has focused on investigations concerning the reduced mechanical and durability performance. Circulation of stray current through conventional steel reinforcement is known to cause accelerated corrosive damage to steel. The discontinuous and discrete nature of steel fibres is believed to be able mitigate against such corrosive damage; however certain knowledge gaps relating to SFRC have become apparent since the construction and operation of the Channel Tunnel when it was first used as the primary railway tunnel lining material.

Electrochemical techniques were used in this work to investigate the pitting corrosion initiation in SFRC under simulated stray current conditions. Voltammetry tests including Tafel and Cyclic Potentiodynamic (CP) polarization tests were conducted on steel fibres embedded in a sponge beam soaking up the simulated concrete pore solution. The simulated concrete pore solution was made from a saturated solution of $Ca(OH)_2$ which has a similar level of chemical concentrations to that of a normal concrete pore solution [19]. NaCl was added into the simulated concrete pore solution to obtain kinetic information about chloride induced corrosion reactions on the electrode (i.e. steel fibre) surface during the Tafel polarization test. The CP polarization test provided additional information on the formation and breakdown of the passive layer on the steel surface subjected to an externally applied potential, such as that induced by stray current. In addition, ~~E~~electrochemical impedance spectroscopy (EIS) was conducted on steel fibres embedded in mortar specimens to investigate the effect of the gap between discrete steel fibres on the electrical conductivity of SFRC. EIS tests also enabled a quantitative study of the electrical conductivity of mortar (or cement paste), which acts as a solid electrolyte during electrochemical reactions. The interpretation of EIS results based on equivalent electronic circuit modelling provides valuable information on charge transfer kinetics such as charge transfer resistance (R_{ct}) which is associated with the local corrosion/pitting of steel. In addition to the electrochemical tests, standard concrete cylinder specimens, with and without steel fibres, were cast in the laboratory to determine the effect of steel fibre contents on the compressive strength of concrete. The mix proportions of mortar and concrete specimens used in this work match those previously used in the Channel Tunnel project as the tunnel lining material [39].

~~2.1.~~2.1 Steel fibre corrosion tests in simulated concrete pore solution

Steel naturally develops an inert passive layer when exposed to an alkaline solution. The alkaline solution in wet concrete is provided by $Ca(OH)_2$, the major cement hydration reaction product. The simulated concrete pore solution was made from a saturated solution of $Ca(OH)_2$ at a room temperature (i.e. approximately 20 °C) using deionized water. A three electrode electrochemical cell (Fig. 3~~-~~(a)), was used in the Tafel and Cyclic Potentiodynamic (CP) polarization tests. The permeation properties and pore structure of concrete were simulated using a sponge beam, soaking up the simulated pore solution. A commercially available cold drawn low carbon steel fibre (Fig. 4), 62 mm in length and 0.75 mm in diameter, was used as the working electrode (WE). The embedded length of the WE into the sponge beam was maintained as 50 mm which gives an exposed surface area of approximately 1.18 cm^2. All steel fibres were tested with their as-received surface conditions and were only flushed with deionized water prior to testing; thus ensuring that the real-life conditions of steel fibres are simulated in the laboratory. A HB pencil graphite electrode, 60 mm in length and 1.2 mm in diameter, was used as the counter electrode (CE) which completes the electrochemical cell circuit. A gap of 10 mm was maintained between the WE and CE during the test. During both CP and Tafel polarization tests, the potential was applied against a silver/silver chloride (Ag/AgCl) reference electrode (RE, with filling solution 3% NaCl) placed on the top surface of the sponge beam. The standard electrode potential of RE is 250 ± 5 mV against a Standard Hydrogen Electrode (SHE).

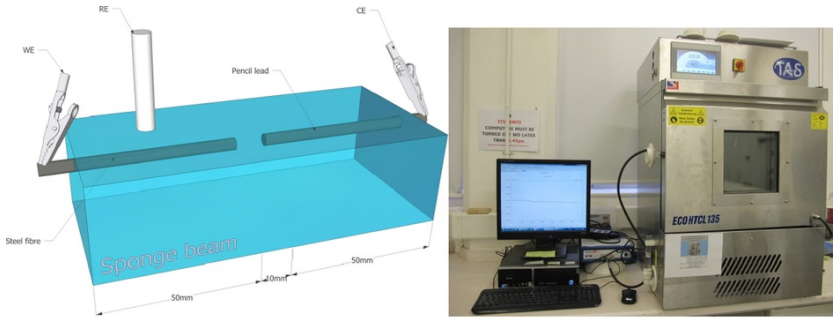

(a) Schematic of the electrochemical cell

(b) Environmental chamber

~~Fig. 3.~~Fig. 3 Electrochemical cell.

alt-text: Fig. 3

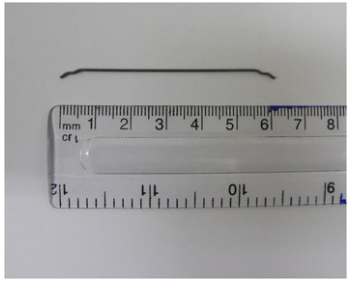

~~Fig. 4.~~Fig. 4 Steel fibre used in this work (DRAMIX 4D 80/60BG).

alt-text: Fig. 4

A Faraday cage is essential for electrochemical analysis conducted at either a low current (e.g. the Tafel polarization test) or a high frequency (e.g. EIS) as they are particularly susceptible to interference from an external electrical field. The electrochemical cell (Fig. 3(a)) was placed inside an environmental chamber (Fig. 3(b)) which was set at a constant temperature (20 °C) and humidity (90%). The exterior and interior parts of the environmental chamber were made from stainless steel and connected to earth; the environmental chamber therefore performs as a Faraday cage and protects the interior from electromagnetic interference from the outside. Cell cables run through a hole in the chamber wall.

The presence of chloride is often associated with the breakdown of the passive layer of steel reinforcement in concrete. To study chloride attack of steel fibres, NaCl was added into the simulated pore solution at different concentrations, i.e. 0, 0.3, 0.6 and 0.8 mol/L, which represent different working conditions from a chloride free condition to a marine environment [34]. Sponge beams were immersed into the simulated solution for 5 ~~minutes~~min before an open circuit potential (OCP) was measured. The Tafel polarization test was then conducted using a Gamry Interface 1000E potentiostat. A small overpotential, ± 250 mV from the OCP, was applied to WE and the current flow between the WE and CE was measured by the potentiostat. A slow potential scanning rate of 1 mV/~~sec~~s was used and this allowed the nonlinear correlation between externally applied potential (E) and the current density i ($i = I/A$). A Tafel slope analysis was then conducted to determine the corrosion current density (i_{corr}) which is discussed in Section 3.2. To investigate the effect of stray current on the corrosion rate (CR) of steel fibres, a constant DC voltage (10 V) was applied to the cell using freshly prepared electrodes and electrolytes. The Tafel polarization test was then conducted and results are discussed in Section 3.2 as well.

The presence of chloride ions in the concrete pore solution can break down the passive layer of steel reinforcement and lead to a localized pitting corrosion. Pitting corrosion, in comparison to uniform corrosion, is more difficult to measure using conventional civil engineering methods such as a weight loss measurement as there is no significant mass change [14]. The pitting tendency of steel fibre was studied in this work through the CP polarization test using the same electrochemical cell (Fig. 3(a)). The CP polarization test was based on the potential sweep mainly along the positive or anodic direction, e.g. ~~-~~ 0.5 V to 1.5 V from the OCP. This enabled the investigation of the passivation behaviour of steel fibres and the breakdown of the passive layer which occurs within the positive or anodic region. The potential sweep was applied to the WE at a scanning rate of 5 mV/~~sec~~s. A reverse scan was then conducted until a hysteresis loop closed or the corrosion potential was reached. The enclosed area by the hysteresis loop was used to qualitatively define the corrosion susceptibility of steel fibre and this is discussed in Section 3.2. Both Tafel and CP polarization tests may change the surface properties of the electrode. Fresh steel fibres, sponge beams and electrolytes were prepared and used in each test. Three parallel samples were prepared and tested to ensure the repeatability of the results.

~~2.2.~~2.2 SFRC mixes

The SFRC mix proportions are shown in Table 1. The coarse aggregate used was 4 ~~-~~ 25 mm graded crushed gravel with a water absorption value of 1.49%. The fine aggregate was well-graded medium sand with a water absorption value of 0.78%. CEM I 52,5 N cement, complying with BS EN 197-1 [44], was used. The same type of steel fibre used in the voltammetry tests was used in concrete mixing. Three mixes with different steel fibre contents, i.e. 0, 20 and 40 kg/m^3, were used to assess the effect of steel fibre contents on the compressive strength of concrete. A 40Fibre mix represents the SFRC mix previously used in the Channel Tunnel project as the lining material [39].

Table 1 SFRC mix proportions.

alt-text: Table 1

Concrete mixes	CEM I 52,5 (kg/m^3)	Free W/C	Sand (0–4 mm) (kg/m^3)	Gravel (4–25 mm) (kg/m^3)	Steel fibre (kg/m^3)	Superplasticizer (kg/m^3)
0Fibre	480	0.35	845	869	0	4.8
20Fibre	480	0.35	845	869	20	4.8
40Fibre	480	0.35	845	869	40	4.8

Both coarse and fine aggregates were oven-dried before mixing and this enabled a good control of the free water content of the mixture. All aggregates were premixed with half the mixing water for about 1 ~~minute~~min. Cement, steel fibre and the remaining mixing water with a poly carboxylate based superplasticizer (Fosroc Auracast 200) were added and mixing was carried out for another 1 ~~minute~~min. The content of superplasticizer, 4.8 kg/m^3, was same as that used in the Channel Tunnel project [39]. Three standard concrete cylinder specimens, 150 mm diameter and 300 mm length, were cast in each mix at an ambient temperature of approximately 20 °C. Within 24 ~~hours~~h of casting, the cylinder specimens were demoulded and placed into a water curing tank set at 20 °C until the compressive strength test was conducted at the age of 28 days. Exposed steel fibres in the concrete specimens, once in direct contact with the welded mesh panel inside the curing tank, may give rise to galvanic corrosion. To prevent such direct contact a plastic sheet was placed between the SFRC specimens and the mesh panel.

~~2.3.~~2.3 Steel corrosion tests in mortar specimens

In comparison to the CP and Tafel polarization tests, only a small perturbation of the current is required by electrochemical impedance spectroscopy (EIS). This makes EIS a non-destructive testing method as the electrochemical properties of the electrolyte (i.e. mortar) and steel do not change significantly during the test. EIS is also an ideal testing method for determination of electrochemical processes occurring in a low conductive electrolyte such as mortar and concrete [11].

In addition to the study of individual fibres, a major focus of this work is the complication of the discrete nature of steel fibres in SFRC and the electrical conductivity of concrete. This was achieved through the EIS tests to mortar (or cement paste) instead of concrete specimens. Mortar (or cement paste) is a cementitious composite between cement, water and sand whereas concrete also contains coarse aggregate such as limestone, gravel or granite. The EIS results obtained from mortar, which performs as a low conductive electrolyte in concrete, can be representative of those obtained from concrete directly. The effect of coarse aggregate on the possible inhomogeneities of concrete subjected to an electrical field is an on-going area of research.

The electrochemical cell is shown in Fig. 5. A steel fibre was embedded into the mortar and used as the WE. Two graphite plates, 40 × 50 × 3 mm, were placed on both sides of the WE as the CE. The exposed area of CE was much bigger than that of the WE and this ensured a uniform transmission of electrical signals [26]. The gap between the WE and CE was maintained as 1 cm which simulated the discontinuity of steel fibres inside concrete. An Ag/AgCl reference electrode (RE) was placed on a wet sponge to achieve a good electrical connection and located approximately 5 mm from the WE to reduce the current resistance drop between the WE and the RE. The mortar specimens were placed in the environmental chamber (Fig. 3(b)) immediately after casting. The environmental chamber was set at 20 °C and 90% humidity. EIS was conducted inside the environmental chamber at an age of 28 days after casting using the Gamry Interface 1000E potentiostat.

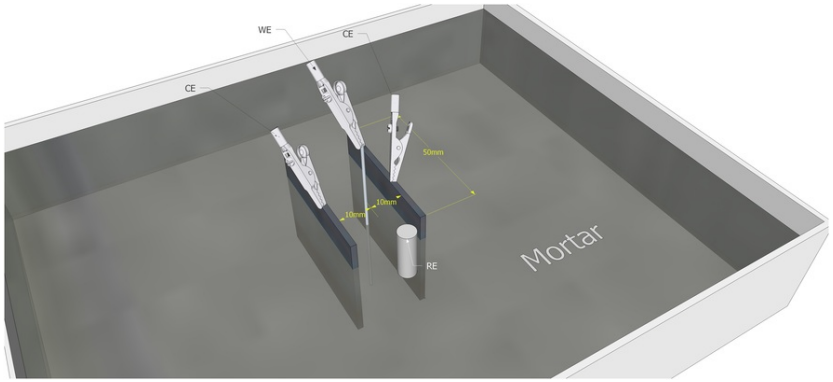

~~Fig. 5.~~Fig. 5 Schematic of the electrochemical cell used in EIS.

alt-text: Fig. 5

(Can this paragraph (only 1 sentence) be combined to the the previous paragraph at the end? Thanks!)EIS was conducted by sweeping an amplitude sinusoidal AC signal (25 mV) with frequencies varying between 10^5 Hz and 10^{-2} Hz.

Table 2 shows the mortar mix proportions used in EIS. The cement content and water cement ratio (W/C) were same as the SFRC mixes (Table 1); this allows the mortar specimens to be representative of the cement paste in SFRC specimens. NaCl was added into the mortar mixes to assess the effect of chloride on the electrical conductivity of mortar (or cement paste). Different NaCl contents, i.e. 0%, 2%, 4% and 6% by mass of cement, were added into the mix to study the electrical conductivity of mortar and the corrosion behaviour of the steel fibre. The impedance of the electrochemical cell was determined as the correlation between the applied potential (E) and the measured current (I). The best fit results based on equivalent electronic circuit modelling are discussed in Section 3.3.

Table 2 Mortar mix proportions.

alt-text: Table 2

Mortar mixes	CEM I 52,5 (kg/m^3)	Free W/C	Sand (0–4 mm) (kg/m^3)	NaCl (kg/m^3)
0%NaCl	480	0.35	1814	0
2%NaCl	480	0.35	1814	9.6
4%NaCl	480	0.35	1814	19.2
6%NaCl	480	0.35	1814	28.8

~~3.~~3 Results and discussion

~~3.1.~~3.1 Compressive strength

The average compressive strength of SFRC was determined at the age of 28 days and results are shown in Fig. 6. The presence of steel fibres contributed to an increase of the 28-day compressive strength. The average compressive strength of 40Fibre mix (i.e. 40 kg/m^3 steel fibre) was 58.6 MPa which is 10% higher than the unreinforced concrete cylinders, 52.4 MPa.

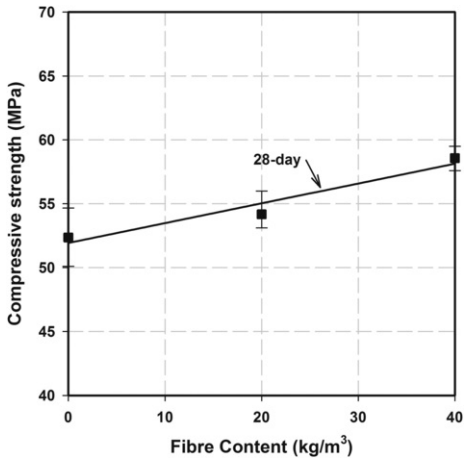

Fig. 6 SFRC compressive strength at the age of 28 days.

alt-text: Fig. 6

~~3.2.~~3.2 Steel fibre corrosion in simulated concrete pore solution

The Tafel polarization test results are presented as Tafel plots, as seen in Fig. 7, where an externally applied potential (E) is plotted against the logarithm of the current density (i_{corr} = I_{corr}/A). A is the area of the exposed surface

of the embedded fibre in the sponge beam. In the anodic polarization region ($E > E_{corr}$), the oxidation of steel led to an exponential increase of I and this agrees with the Tafel behaviour as discussed previously. It should be noted that corrosion current (I_{corr}) and the corrosion current density (i_{corr}) can also be obtained by extrapolating the linear portions of the anodic and cathodic Tafel polarization plots to their intersection. This graphical method however may lead to significant observational error and has not been used in this work. A nonlinear regression analysis or Tafel slope analysis, based on Butler-Volmeter equation (Eq. (11)), was conducted using Gamry Echem Analyst software [45]. The best fit curves are also shown in Fig. 7 and the best fit parameters, including E_{corr}, i_{corr}, β_a and β_c, are presented in Table 3. The corrosion rate (CR) was calculated according to Eq. (6) and presented in Table 3 too. The effect of chloride on the i_{corr} and thus the CR was less significant when the chloride concentration was ~~less than~~ ≤ 0.6 mol/L, although a decrease in the corrosion potential (E_{corr}) was observed in the presence of chloride. At a higher chloride centration (i.e. 0.8 mol/L), both the i_{corr} and CR increased by one order of magnitude in comparison to those obtained from the chloride free solution and this indicates a high risk of pitting corrosion.

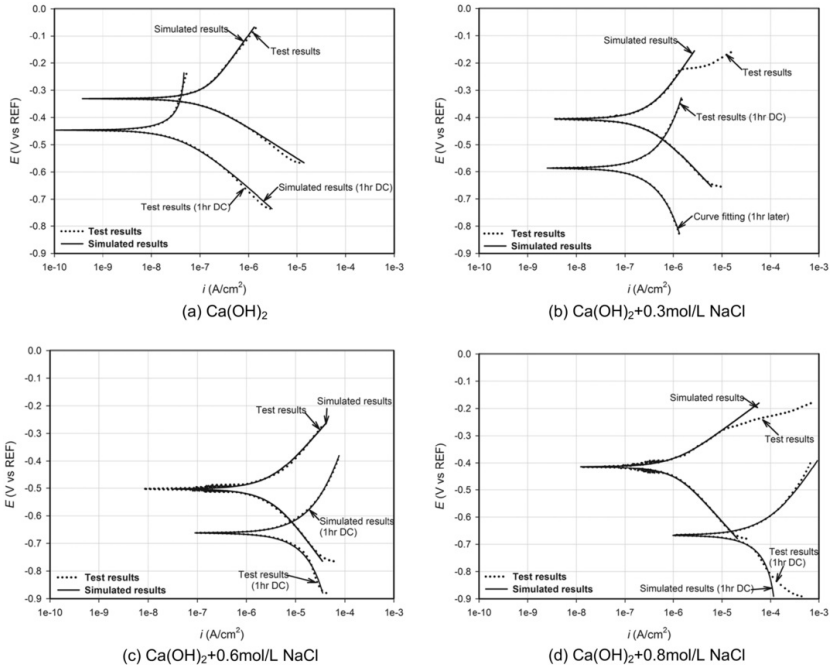

Fig. 7 Tafel polarization results.

alt-text: Fig. 7

Table 3 Tafel polarization results (0 ~~hour~~ h DC).

alt-text: Table 3

Electrolyte	E_{corr} (mV)	β_a (V/dec)	β_c (V/dec)	i_{corr} (μA/cm²)	CR (mm/year)
$Ca(OH)_2$	-- 331	0.221	0.134	0.096	0.001
$Ca(OH)_2$ + 0.3 mol/L NaCl	-- 406	0.232	0.187	0.246	0.003
$Ca(OH)_2$ + 0.6 mol/L NaCl	-- 503	0.193	0.229	0.266	0.003
$Ca(OH)_2$ + 0.8 mol/L NaCl	-- 415	0.132	0.200	0.981	0.011

To investigate the effect of stray current on the corrosion behaviour of steel fibres, a constant DC voltage (10 V) was applied through the steel fibre (anode) and the graphite rod (cathode) using freshly prepared

electrochemical cells. Tafel polarization tests were then conducted and results are shown in Fig. 7. Corrosion potential (E_{corr}) was found to shift more negatively due to the exposure to the DC voltage. The application of the DC voltage however did not affect the i_{corr} and CR in the simulated solutions containing up to 0.6 mol/L NaCl. This indicates that steel fibres had developed the passivation layer under alkaline conditions. This finding is also justified by the Tafel slope analysis and the best fit parameters as presented in Table 4; i_{corr} and the CR were not significantly affected with up to 0.6 mol/L NaCl added into the solution. The chloride induced corrosion was higher when the chloride concentration was 0.8 mol/L; i_{corr} increased by almost 3 orders of magnitude in comparison to that obtained for the chloride free simulated solution. This indicates that serious pitting corrosion, associated with the breakdown of the passivation layer, had developed on the electrode surface at such a high chloride concentration. 0.6 mol/L can therefore be taken as the chloride threshold level for corrosion of steel fibres in the simulated concrete pore solution. This chloride threshold value is higher than that assessed for conventional steel reinforcement in the simulated concrete solution, i.e. 0.17–0.34 mol/L [46], which indicates the steel fibre has a higher resistance to chloride attack.

Table 4 Tafel polarization results (1 ~~hour~~ h DC).

alt-text: Table 4

Electrolyte	E_{corr} (mV)	β_a (V/dec)	β_c (V/dec)	i_{corr} (μA/cm^2)	CR (mm/year)
$Ca(OH)_2$	–446	0.620	0.159	0.034	0.0004
$Ca(OH)_2$ + 0.3 mol/L NaCl	–588	0.398	0.447	0.354	0.004
$Ca(OH)_2$ + 0.6 mol/L NaCl	–662	0.419	0.525	16.86	0.197
$Ca(OH)_2$ + 0.8 mol/L NaCl	–666	0.283	0.301	81.44	0.953

The corrosion current densities (i_{corr}) presented in Table 3 and Table 4 are based on the Tafel kinetics of individual redox reactions (i.e. Eqs. (3), (4) and (5)). To study the formation of the passivation layer and the corrosion behaviour of steel fibres under stray current environments, CP polarization tests were conducted on the same corrosion cells (Fig. 3) using freshly prepared electrodes and electrolytes. CP polarization test results (Fig. 8) show a sudden decrease of the current density (i) with an increase of the potential (E) which can be defined as a passivation potential (i.e. E_{pass}). E_{pass} represents the potential value at which the passive layer is developed on the surface of the electrode. With a further increase of E, i increased further and this can be attributed to the breakdown of the passive layer. The current value increased sharply from the pitting potential (E_{pit}) where the disruptive effect of chloride ions overcame the stabilizing effect of hydroxide ions [30]. A reverse scan was then conducted until the hysteresis loop closed or the corrosion potential was reached. The area enclosed by the hysteresis loop was used to qualitatively define the corrosion susceptibility, i.e. a bigger enclosed area indicates a lower corrosion susceptibility [35]. From visual observation, the enclosed area does not change significantly with up to 0.6 mol/L NaCl added into the simulated solution. In addition to E_{pit}, ΔE, the passive potential range or the difference between E_{pit} and E_{pass} (i.e. E_{pit} - E_{pass}), also represents the pitting tendency of the electrode according to Popov [11]. There is no obvious decrease in ΔE with up to 0.6 mol/L NaCl added to the simulated solution and a constant ΔE value of 1.0 V (vs the Ag/AgCl reference electrode) was achieved. At a high chloride concentration, 0.8 mol/L, ΔE reduced to 0.6 V and this shows a high risk of pitting corrosion. This finding agrees with the chloride threshold level estimated through the Tafel polarization test. This can be attributed to the chloride induced depassivation of the passive layer on the electrode surface, despite being under alkaline conditions [30]. The cyclic polarization curves also experience a sharp decrease in the measured current before the hysteresis loop is closed during the reverse scan. This is called a protection potential (E_{pro}) [11] which is close in value to E_{corr}.

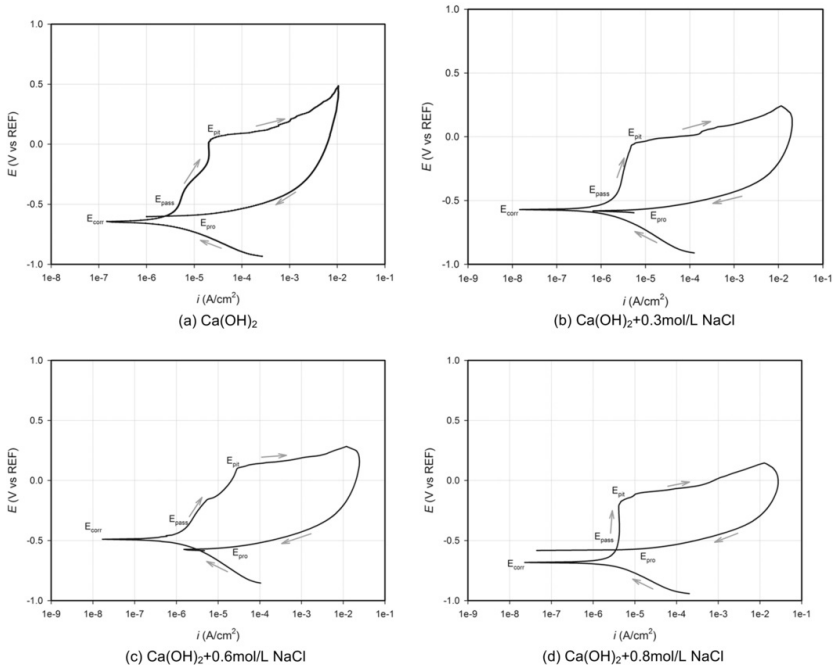

~~Fig. 8.~~Fig. 8 CP curves.

alt-text: Fig. 8

Tafel polarization tests determine the corrosion current density (i_{corr}) and thus the corrosion rate (CR) at an equilibrium state between the anodic and cathodic reactions which are both kinetically controlled and obey Eqs. (9) and (10). This is generally applicable for steel reinforcement in a passive corrosion state. During CP polarization tests, the externally applied potential (E) further pushes the anodic potential away from the equilibrium potential which accelerates the anodic reaction or the corrosion rate. CP polarization tests enabled the study of depassivation of steel fibres due to the combined effect of chloride and externally applied DC current. The latter can be taken as an estimation of the stray current effect. A high chloride concentration, 0.8 mol/L, decreased the resistance of steel fibre to stray-current induced corrosion by reducing the ΔE value.

Wet sponge beams were used to represent concrete in both Tafel and CP polarization tests. As the electrical conductivity of a wet sponge beam differs from cement paste in concrete, it is necessary to justify if the cement paste may become a barrier for a continuous path (circuit) of discrete steel fibres in SFRC. Glass and Buenfeld [47] reported that part of the bound chloride also presents a corrosion risk to the embedded steel due to a 'chloride reservoir' effect at the steel-concrete interface. The chloride threshold level determined using the equivalent concrete pore solution may therefore need further justification in order to predict the chloride threshold level. This was achieved in this work through the EIS investigation on steel fibres embedded in mortar specimens.

~~3.3.~~3.3 Electrical conductivity of mortar (cement paste)

Electrochemical impedance spectroscopy (EIS) was used to assess the electronic conductivity of mortar (or cement paste) which performs as a solid electrolyte in reinforced concrete. EIS data were presented as a Bode phase plot (Fig. 9 (a)), a Bode $|Z|$ plot (Fig. 9 (b)) and a Nyquist plot (Fig. 9 (c)). The Bode phase plot allows the phase shift angle (θ) to be plotted with regards to the excitation frequency (Hz) in a logarithmic scale. The Bode $|Z|$ plot allows the absolute values of the impedance ($|Z|$) to be plotted against the logarithm of frequency (Hz). The Nyquist plot (Fig. 9 (c)) allows the imaginary resistance ($\dot{Z}$) to be plotted against the real resistance ($\dot{Z}$). Each dot in the Nyquist plot represents the impedance measured at an excitation frequency. The correlations between $|Z|$, $\dot{Z}$, $\dot{Z}$ and θ are defined by Eqs. (15) and (16) [48].

$$|Z| = \sqrt{(Z')^2 + (Z'')^2} \quad \textbf{(15)}$$

$$\tan\theta = \frac{Z''}{Z'} \quad \textbf{(16)}$$

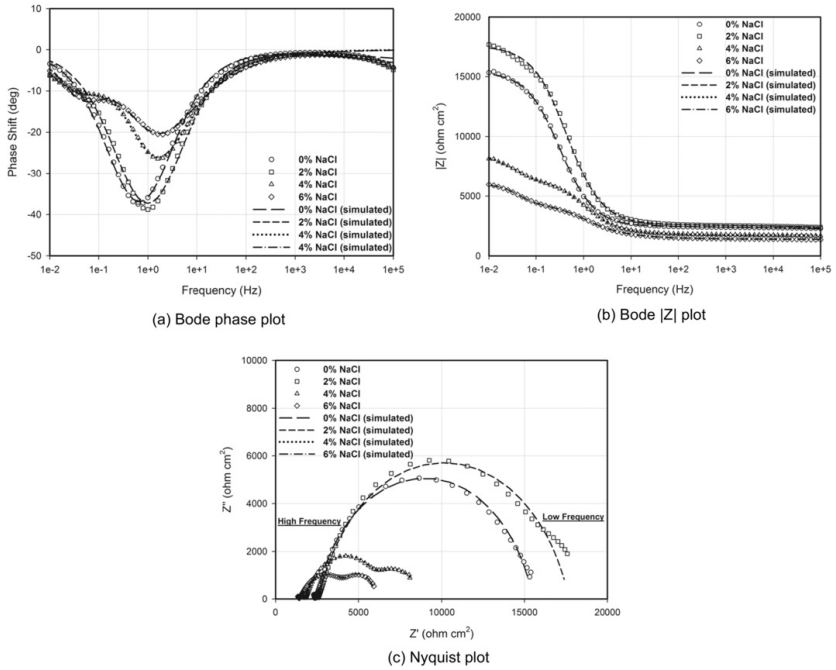

~~Fig. 9.~~**Fig. 9** 28-day mortar EIS results.

alt-text: Fig. 9

With up to 2% NaCl added to the mix, the Bode phase plot (Fig. 9(a)) shows that the phase angle (θ) drops constantly at low frequencies until the lowest value (valley) was reached at an excitation frequency of 0.8 Hz. This indicates that the steel fibre was in a local or pitting corrosion state [26]. With 4% and 6% NaCl added to the mix, two valleys were identified at 0.05 and 1.8 Hz respectively. This shows an accelerated corrosion extent where the corrosion was controlled by the mass transfer through the steel/concrete interface [26]. With up to 2% NaCl (by mass of cement) added to the mix, the Bode $|Z|$ plot (Fig. 9(b)) also shows that there is no significant difference in total impedance, $|Z|$, especially at low frequencies. There is however a major decrease of | Z | from above 15,000 ~~ohm~~ Ω·cm^2 to 8,000 ~~ohm~~ Ω·cm^2 at a higher NaCl content of 4%.

Two equivalent electronic circuits (Fig. 10) were proposed to represent the above two different corrosion extents, i.e. from local or pitting corrosion to constant corrosion reactions controlled by the mass transfer. A Warburg diffusion element was created in the second circuit (Fig. 10(b)) to represent the constant corrosion controlled by the mass transfer. In the Nyquist plot (Fig. 9(c)), the real impedance (Z') within the high frequency region is primarily due to the cell's solution resistance (or the bulk resistance of concrete) and this is represented as a resistor R_s in the electronic circuit (Fig. 10). The membrane resistance (R_f) and charge transfer resistance (R_{ct}) represent the resistance of the passive layer and the charge transfer resistance of the electrode and surrounding electrolyte (i.e. mortar or cement paste) [49]. R_{ct} and R_f define the difficulty of a kinetically controlled electrochemical reaction. The capacitance of the passive layer developed on the steel surface was represented by a capacitor (C_f). The electrical double layer between the electrode and electrolyte was modelled as a capacitor (C_{dl}) as well. A constant phase element (CPE), rather than a standard capacitor, was used in the equivalent circuits to model C_f and C_{dl}, as it can better consider the surface roughness and heterogeneousness of a double layer [49]. When the positively charged ferrous ions are diffused into the solution as a result of the electrolysis reactions, they may affect the conductivity of the whole system by creating a diffusion barrier [50].

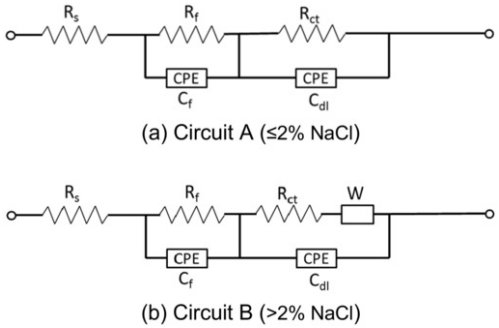

~~Fig. 10.~~**Fig. 10** Equivalent circuit models.

alt-text: Fig. 10

Best fit curves based on the equivalent electronic circuit modelling were obtained using Gamry Echem Analyst software [45]. The equivalent circuit simulation results match very well with the original EIS data as shown in Fig. 9. EIS best fitting results (Table 5) indicate that the presence of NaCl did not further increase the solution resistance (R_s) or the electrical conductivity of the mortar (or cement paste). With 2% NaCl added into the mix, the changes in the best fit parameters, i.e. R_f, C_{dl} and R_{ct}, were insignificant. With 4% NaCl added into the mix, R_{ct} reduced from above 10 kΩ·cm^2 to 1.7 kΩ·cm^2. This indicates a high susceptibility for steel pitting corrosion; an increase in the corrosion rate (CR) is very much expected according to Eq. (13). Table 5 indicates that R_f is much smaller than R_{ct} and this can be attributed to the chloride induced depassivation effect [49]. In addition to R_{ct} and R_f, a significant increase in C_{dl} was identified, especially at high NaCl contents of 4% and 6%. This indicates that constant corrosion had occurred on the steel surface [49] and this finding agrees with the interpretation of the Bode plot (Fig. 9 (a)) as discussed previously. In summary, 4% NaCl (by mass of cement) can be taken as the chloride threshold level for corrosion of steel fibres in mortar which is much higher than that of conventional steel reinforcement, i.e. between 0.15% and 0.6% [31]. Mortar, as a solid electrolyte, also led to a better corrosion resistance to chloride in comparison to the results obtained using the simulated concrete pore solution, as discussed in Section 3.2.

Table 5 EIS best fitting results (28-days).

alt-text: Table 5

Mortar sample	R_s (kΩ·cm^2)	R_f (kΩ·cm^2)	C_f (10^{-6}S·s^n·cm^{-2})	n_f	R_{ct} (kΩ·cm^2)	C_{dl} (10^{-6}S·s^n·cm^{-2})	n_{dl}	W (10^{-3}SE·s$^{1/2}$·cm^{-2})
0%NaCl	1.5	1.0	6.4	0.29	13.0	57.5	0.84	-
2%NaCl	0.99	1.6	1.4	0.34	15.0	38.1	0.83	-
4%NaCl	1.7	2.4	65.6	0.99	6.0	331.8	0.45	20.4
6%NaCl	1.4	0.9	120.1	1.00	5.0	312.0	0.41	40.7

~~4.~~4 Conclusion

The corrosive damage due to stray current will become more prominent as the UK government is committed to developing more electric rail networks to provide sustainable and cleaner services for the public. Steel fibre reinforced concrete (SFRC) represents a potential solution to this problem. This paper investigates the corrosion behaviour of steel fibres in simulated concrete pore solutions through Tafel and Cyclic Potentiodynamic (CP) polarization tests. The presence of high concentration chloride ions (i.e. ≥ 0.6 mol/L) was found to increase the pitting tendency of steel fibres and 0.6 mol/L may be taken as the chloride threshold level for corrosion of steel fibres in the simulated concrete pore solution. The ~~C~~corrosion behaviour of steel fibres in concrete was investigated through electrochemical impedance spectroscopy (EIS). Correlation of the EIS data and the best fit results with the equivalent electronic circuits indicate that SFRC demonstrates a higher corrosion resistance in comparison to conventional steel reinforcement and 4% NaCl (by mass of cement) can be taken as the chloride threshold level for corrosion of steel fibres in concrete.

References

[1] R. Kemp, Traction energy metrics, In: *Rail Safety and Standards Board,* 2007, Lancaster University; UK.

[2] P. Keen and R. Phillpotts, Low ~~e~~Cost ~~e~~Electrification for ~~b~~Branch ~~l~~Lines, 2010, DeltaRail; Derby.

[3] M. Niasati and A. Gholami, Overview of stray current control in DC railway systems, In: *Railway Engineering - Challenges for Railway Transportation in Information Age,* 2008, ICRE; Hong Kong, 1–6.

[4] W. Li, The monitor and control system of stray current corrosion in metro, In: *Urban Mass Transit,* **6**, 2003, 48–52.

[5] L. Bertolini, M. Carsana and P. Pedeferri, Corrosion behaviour of steel in concrete in the presence of stray current, ~~*Corrosion Science*~~*Corros. Sci.* **49**, 2007, 1056–1068.

[6] P. Vernon, Stray-current corrosion control in metros, *Proc. Inst. Civ. Eng.* **80**, 1986, 641–650.

[7] S.J. Duranceau, W.J. Johnson and R.J. Pfeiffer-Wilder, A study examining the effect of stray current on the integrity of continuous and discontinuous reinforcing bars, ~~*Experimental Techniques*~~*Exp. Tech.* **35**, 2011, 53–58.

[8] National Physical Laboratory (UK), Estimate of annual costs attributable to corrosion of reinforced concrete structures in the United Kingdom, www.npl.co.uk, 2015, Accessed 18 November 2016.

[9] BSI, BS EN 50122-2:2010 Railway Applications - Fixed Installations - Electrical Safety, Earthing and the Return Circuit, 2010, British Standards Institution.

[10] Parsons Brinckerhoff, TCRP ~~r~~Report 155: ~~t~~Track ~~d~~Design ~~h~~Handbook for ~~l~~Light ~~r~~Rail ~~t~~Transit, 2012, Transportation Research Board; U.S.A..

[11] B. Popov, Corrosion Engineering: Principles and Solved Problems, 2015, Elsevier Science Ltd.

[12] Gamry, Application note: getting started with electrochemical corrosion measurement, http://www.gamry.com/application-notes/corrosion-coatings/basics-of-electrochemical-corrosion-measurements/, 2015, Accessed 2 April 2016.

[13] ASTM, G102-89 Standard ~~p~~Practice for ~~e~~Calculation of ~~e~~Corrosion ~~r~~Rates and ~~r~~Related ~~i~~Information From ~~e~~Electrochemical ~~m~~Measurements, 1999, American Society for Testing and Materials; West Conshohocken, PA.

[14] Metrohm, Autolab application note part 2: measurement of corrosion rates, http://www.ecochemie.nl/Applications/, 2011, Accessed 1 December 2016.

[15] J. Wang, Analytical ~~e~~Electrochemistry, 2000, Wiley-VCH; New York, USA.

[16] C. Cao, Principles of ~~e~~Electrochemistry of ~~e~~Corrosion, 2008, Chemical Industry Press; Beijing, China.

[17] A.C. Fisher, Electrode Dynamics (Oxford Chemistry Primers), 1996, Oxford University Press.

[18] M. Stern and A.L. Geary, Electrochemical polarization I. a theoretical analysis of the shape of polarization curves, *Electrochem. Soc.* **104**, 1957.

[19] D.G. John, P.C. Searson and J.L. Dawson, Use of AC impedance technique in studies on steel in concrete in immersed conditions, ~~*British Corrosion Journal*~~*Br. Corros. J.* **16**, 1981, 102–106.

[20] A.M. Aguirre-Guerrero, R. Mejía-De-Gutiérrez and M.J.R. Montês-Correia, Corrosion performance of blended concretes exposed to different aggressive environments, ~~*Construction and Building Materials*~~*Constr. Build. Mater.* **121**, 2016, 704–716.

[21] S. Ahmad, M.A.A. Jibran, A.K. Azad and M. Maslehuddin, A simple and reliable setup for monitoring corrosion rate of steel rebars in concrete, *Sci. World J.* **2014**, 2014.

[22] W. Aperador, E. Ruíz and A. Delgado, Electrochemical impedance spectroscopy analysis on steel embedded in a concrete alkali exposed on the chloride media, *Int. J. Electrochem. Sci.* **9**, 2014, 7506–7517.

[23] B. Dong, Q. Qiu, J. Xiang, C. Huang, F. Xing and N. Han, Study on the carbonation behavior of cement mortar by electrochemical impedance spectroscopy, *Materials* **2014**, 2014, 218–231.

[24] D.V. Ribeiro and J.C.C. Abrantes, Application of electrochemical impedance spectroscopy (EIS) to monitor the corrosion of reinforced concrete: a new approach, ~~*Construction and Building Materials*~~*Constr. Build. Mater.* **111**, 2016, 98–104.

[25] D.V. Ribeiro, C.A.C. Souza and J.C.C. Abrantes, Use of Electrochemical Impedance Spectroscopy (EIS) to monitoring the corrosion of reinforced concrete, *IBRACON Struct. Mater. J.* **8**, 2015, 529–546.

[26] J. Wei, X.X. Fu, J.H. Dong and W. Ke, Corrosion evolution of reinforcing steel in concrete under dry/wet cyclic conditions contaminated with chloride, ~~*Journal of Materials Science and Technology*~~*J. Mater. Sci. Technol.* **28**, 2012 905–912.

[27] Gamry, Application note: basics of electrochemical impedance spectroscopy, http://www.gamry.com/application-notes/corrosion-coatings/basics-of-electrochemical-corrosion-measurements/, 2015, Accessed 2 April 2016.

[28] Metrohm, Autolab application note EIS01: electrochemical impedance spectroscopy (EIS), http://www.ecochemie.nl/Applications/, 2011, Accessed 1 December 2016.

[29] A.M. Neville, Properties of ~~c~~Concrete, 2011, Pearson Education Limited; England.

[30] M. Saremi and E. Mahallati, A study on chloride-induced depassivation of mild steel in simulated concrete pore solution, ~~*Cement and Concrete Research*~~*Cem. Concr. Res.* **32**, 2002, 1915–1921.

[31] ACI, Building Code Requirements for Structural Concrete (ACI 318-08) and Commentary, 2008, American Concrete Institute; Farmington Hills, U.S.A..

[32] RILEM, RILEM TC 178-TMC: Testing and ~~m~~Modelling ~~c~~Chloride ~~p~~Penetration in ~~c~~Concrete, 2002.

[33] X. Wan, F.H. Wittmann, T. Zhao and H. Fan, Chloride content and pH value in the pore solution of concrete under carbonation, *J. Zheijang Univ.* **14**, 2012, 71–78.

[34] J. Shi, W. Sun, J. Jiang and Y. Zhang, Influence of chloride concentration and pre-passivation on the pitting corrosion resistance of low-alloy reinforcing steel in simulated concrete pore solution, ~~*Construction and Building Materials*~~*Constr. Build. Mater.* **111**, 2016, 805–813.

[35] R.D. Moser, P.M. Singh, L.F. Kahn and K.E. Kurtis, Chloride-induced corrosion resistance of high-strength stainless steels in simulated alkaline and carbonated concrete pore solutions, ~~*Corrosion Science*~~*Corros. Sci.* **57**, 2012, 241–253.

[36] H. Sadeghi-Pouya, E. Ganjian, P. Claisse and K. Muthuramalingam, Corrosion durability of high performance steel fibre reinforced concrete, In: T.N. Peter Claisse, (Ed), *The 3rd ~~i~~International ~~c~~Conference on ~~s~~Sustainable ~~c~~Construction ~~m~~Materials and ~~t~~Technologies, Kyoto, Japan,* 2013.

[37] D. Nemegeer, J. Vanbrabant and H. Stang, Brite Euram program on steel fibre concrete subtask: durability: corrosion resistance of cracked fibre reinforced concrete, In: B.S.A.L. Vandewalle, (Ed), *International RILEM Workshop on Test and Design Methods for Steel Fibre Reinforced Concrete,* 2003, RILEM Publications SARL, 47–66.

[38] G. Velayutham and C.B. Cheah, The effects of steel fibre on the mechanical strength and durability of steel fibre reinforced high strength concrete (SFRHSC) subjected to normal and hygrothermal curing, In: *Building Surveying and Technology Undergraduate Conference, BUSTUC 2013, May 31, 2013~~–~~ June 1, 2013,* 2014, EDP Sciences; Langkawi, Malaysia.

[39] A. Caratelli, B.D. Rivaz, A. Meda and Z. Rinaldi, Full-scale tests on precast tunnel segments in fiber reinforced concrete, In: D. Kolić, (Ed), *ITA World Tunnel Congress 2015 Promoting Tunnelling in SEE Region,* 2015, UBITG; Dubrovnik, Croatia.

[40] M.D. Prisco, R. Felicetti, P.G. Gambarova and C. Failla, On the fire behavior of SFRC and SFRC structures in tension and bending, In: A.E.N.A.H.W. Reinhardt, (Ed), *International Workshop High Performance Fiber Reinforced Cement Composites,* 2003, RILEM Publications SARL, 205–220.

[41] M. Burgess and H. Davies, Channel tunnel rail link section 2: Thames tunnel, *Proc. Inst. Civ. Eng. Civ. Eng.* **160**, 2007, 14–18.

[42] A.O.S. Solgaard, M. Carsana, M.R. Geiker, A. Kuter and L. Bertolini, Experimental observations of stray current effects on steel fibres embedded in mortar, ~~*Corrosion Science*~~*Corros. Sci.* **74**, 2013, 1–12.

[43] L. Lin, MSc ~~t~~Thesis: ~~s~~Study of the ~~i~~Influence to the ~~s~~Steel ~~f~~Fiber ~~c~~Concrete ~~d~~Durability ~~d~~Due to the ~~s~~Stray ~~c~~Current, 2005, China University of Mining and Technology; Beijing.

[44] BSI, BS EN 197-1:2011 Cement Part 1: Composition, Specifications and Conformity Criteria for Common Cements, 2011, British Standards Institution.

[45] Gamry, Gamry Echem Analyst 6.32, U.S.A., 2016.

[46] U. Angst, B. Elsener, C.K. Larsen and Ø. Vennesland, Critical chloride content in reinforced concrete - a review, ~~*Cement and Concrete Research*~~*Cem. Concr. Res.* **39**, 2009, 1122–1138.

[47] G.K. Glass and N.R. Buenfeld, The presentation of the chloride threshold level for corrosion of steel in concrete, ~~*Corrosion Science*~~*Corros. Sci.* **39**, 1997, 1001–1013.

[48] Gamry, Physical Electrochemistry & Equivalent Circuit Elements, (in, U.S.)2016.

[49] C.Q. Ye, R.G. Hu, S.G. Dong, X.J. Zhang, R.Q. Hou, R.G. Du, C.J. Lin and J.S. Pan, EIS analysis on chloride-induced corrosion behavior of reinforcement steel in simulated carbonated concrete pore solutions, ~~*Journal of Electroanalytical Chemistry*~~*J. Electroanal. Chem.* **688**, 2013, 275–281.

[50] V. Freger, Diffusion impedance and equivalent circuit of a multilayer film, ~~*Electrochemistry communications*~~*Electrochem. Commun.* **7**, 2005, 957–961.

Highlights

- Formation of stray-current and its effect on the corrosion behaviour of steel fibre reinforced concrete;
- The use of simulated concrete pore solutions as the electrolyte to investigate the corrosion behaviour of steel reinforcement in concrete;

Queries and Answers

Query:

Your article is registered as a regular item and is being processed for inclusion in a regular issue of the journal. If this is NOT correct and your article belongs to a Special Issue/Collection please contact v.william@elsevier.com immediately prior to returning your corrections.

Answer: Yes

Query:

Please confirm that given names and surnames have been identified correctly and are presented in the desired order, and please carefully verify the spelling of all authors' names.

Answer: Yes

Query:

The author names have been tagged as given names and surnames (surnames are highlighted in teal color). Please confirm if they have been identified correctly.

Answer: Yes

Query:

An e-mail address is mandatory for corresponding author; however, private e-mail addresses (e.g., gmail, hotmail, yahoo) should not be included. Please check if an alternative institutional e-mail address can be provided for the corresponding author.

Answer: Can I use both my gmail and university email addresses? Thanks! kangkangtang@gmail.com; k.tang@wlv.ac.uk

Query:

Highlights should consist of 3–5 bullet points (with a maximum of 125 characters per bullet point, including spaces). However, only 2 points were provided, and the characters exceeded the maximum requirement. Kindly provide the necessary corrections. For more information, please see the Guide for Authors.

Answer: Formation of stray-current and its effect on the corrosion behaviour of conventional steel reinforced concrete;
The use of simulated concrete pore solutions to investigate the corrosion behaviour of steel fibre reinforced concrete;
The pitting tendency of steel fibres in steel fibre reinforced concrete (SFRC).

Query:

Please check if the captured keywords are correct and amend as necessary.

Answer: The first key word shall be "Steel fibre reinforced concrete"